CHAPTER 3
RESULT AND DISSCUSION

The investigation of the effect of different factors on retention and separation of some inorganic anions by ion interaction reversed-phase high performance liquid chromatography was done through the variations of the types and concentrations of ion interaction reagent and organic modifier, pH and flow rate of the mobile phase and the wavelength of detection. The results of such investigation could be discussed in the following sections.

3.1 Nature of ion interaction chromatographic separation of anions

Once the mixture of anion standards containing 5 ppm each of IO_3^-, BrO_3^-, NO_3^-, I^- and SCN^- was injected into the chromatographic system. The chromatographic condition employed was 5.0 mM heptylamine-phosphate, 5% (v/v) MeOH, pH 6.4±0.3, flow rate 0.5 mL/min as a mobile phase and detection wavelength at 200 nm. The data of retention times and peak areas are shown in **Table 3.1.** The chromatogram of anions is shown as **Figure 3.1.**

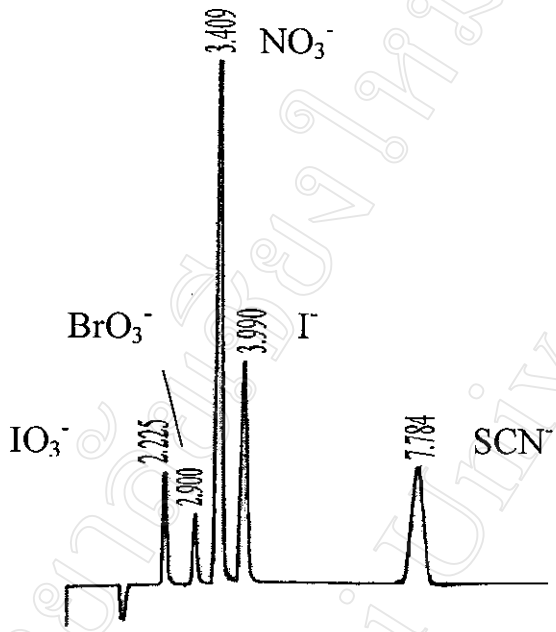

Figure 3.1 Chromatogram of mixed anions standard.

Table 3.1 Retention times and peak areas of anions obtained using a mobile phase of 5.0 mM heptylamine-phosphate, 5% MeOH at pH 6.4±0.3, a flow rate of 0.5 mL/min and 200 nm as a wavelength of detection

Anion	Retention time (min)	Peak area (arbitrary unit)
IO_3^-	2.225	586378
BrO_3^-	2.900	433824
NO_3^-	3.409	3537634
I^-	3.990	1675710
SCN^-	7.784	1944866

The order of elution of anions from the column is in the sequence of IO_3^-, BrO_3^-, NO_3^-, I^- and SCN^-. This elution behavior can be described by electrostatic force that occurs between the analyte ions and ion interaction reagent which is already adsorbed on the stationary phase. The ion pair formed with less electrostatic attraction should be eluted from the column faster. Electrostatic force is dependent directly on the charge of ion, but these anions were chosen by a criterion that they were likely to be singly negatively charged inorganic anions. Electrostatic force is dependent reciprocally on the size of the hydrated analyte ion. The size (free ionic radii) of the interested ions used in this work are shown from the smaller to the bigger, as follows ; IO_3^- (1.83 °A), NO_3^- (1.89 °A), BrO_3^- (1.91 °A), SCN^- (1.95 °A) and I^- (2.06 °A) [47]. Therefore, elution order should be expected to be as IO_3^-, NO_3^-, BrO_3^-, SCN^- and I^-, respectively.

However, from the experiment of which I^- was eluted before SCN^-, this could be explained that even though I^- is bigger than SCN^- but their ionic and molecular shapes are quite different. Their molecular shapes would play important role on the retention behavior. Due to the structure of SCN^- that consists of 3 atoms resulting in linear shape structure, while I^- is a single ion and its structure is spherical. The charge distribution of I^- (spherical shape) is more even than SCN^- (linear shape). Therefore, the hydration of I^-would be more readily formed and its hydrated size would eventually be bigger.

For the case of, BrO_3^- which was eluted before NO_3^-, due to the structure of BrO_3^- that consists of 4 atoms and Br central atom posses one set of lone pair electron resulting in trigonal pyramidal shape structure; while NO_3^- also comprises 4 atoms with no lone pair electron at central atom, therefore its structure is triangular planar shape. The charge distribution of BrO_3^- (trigonal pyramidal shape) is more even than NO_3^- (triangular planar shape). Therefore, the hydration of BrO_3^- would be more readily formed and its hydrated size would eventually be bigger.

The elution mechanism can also be explained following the model of Bidlingmeyer *et al.* [18]. Their explanation on ion interaction chromatographic phenomenon was not based only on ion chromatographic principle, but they also proposed the dynamic equilibrium model to explain this elution mechanism. There are various forces affecting on the interaction mechanism, namely, eluophobic force, eluophilic force, adsorbophobic force and adsorbophilic force and also original electrostatic force. Therefore, elution feature of each analyte ion is practically dependent on their "like dissolves like" properties of either mobile phase or stationary phase, and also electrostatic force of their ion pair formed.

3.1.1 Types of ion interaction reagent

Three types of ion interaction reagent were used in the separation of anions namely; phosphate salts of hexylamine ($CH_3(CH_2)_5NH_2$), heptylamine ($CH_3(CH_2)_6NH_2$) and octylamine ($CH_3(CH_2)_7NH_2$). The standard mixture containing 5 ppm each of IO_3^-, BrO_3^-, NO_3^-, I^- and SCN^- was injected into the ion interaction chromatographic system. The injection volume was 20 μL. The mobile phase used was the mixture of 5.0 mM alkylamine-phosphate with 5% (v/v) MeOH at pH 6.4±0.3 with a flow rate of 0.5 mL/min and wavelength of detection was set at 200 nm

Table 3.2 and **Figure 3.2-3.4**, shows the retention times and peak areas for a mixture of IO_3^-, BrO_3^-, NO_3^-, I^- and SCN^-, and **Table 3.3** show the resolution (R_S) for each of anion pairs recorded under the same condition. By comparing the use of three different ion interaction reagents in the form of phosphate salt of hexylamine, heptylamine and octylamine, it was found that the hexylamine gave the shortest analysis time followed by heptylamine and octylamine. Eventhough the hexylamine seemed to give enough separation between components but the resolution (R_S) between each pair of anions was less than 1.5, except the pair of iodide and thiocyanate ions. While heptylamine and octylamine yielded the resolution of greater than 1.5 for all adjacent pairs which indicated that the separation between components was adequate, but octylamine gave a longer analysis time than heptylamine. So heptylamine is appropriate to be used as an ion interaction reagent because it offers a shorter retention with good resolution among anions compare to hexylamine and octylamine. Therefore, it can be concluded that the type of ion interaction reagent affects the separation in the fashion that the longer the alkyl chain , the longer the retention times. This observation is quite obvious due to the fact that long hydrocarbon chain provides more hydrophobicity which results the ion pair of a particular ion to be better partitioning into the nonpolar octadecyl stationary phase.

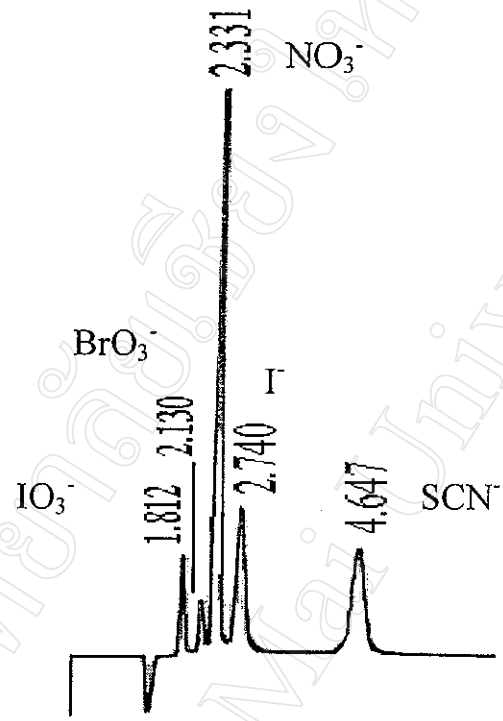

Figure 3.2 Chromatogram of anions obtained using the mobile phase of 5.0 mM hexylamine-phosphate, 5% (v/v) MeOH at pH 6.4±0.3 with a flow rate of 0.5 mL/min and 200 nm as a detection wavelength.

ลิขสิทธิ์มหาวิทยาลัยเชียงใหม่
Chiang Mai University

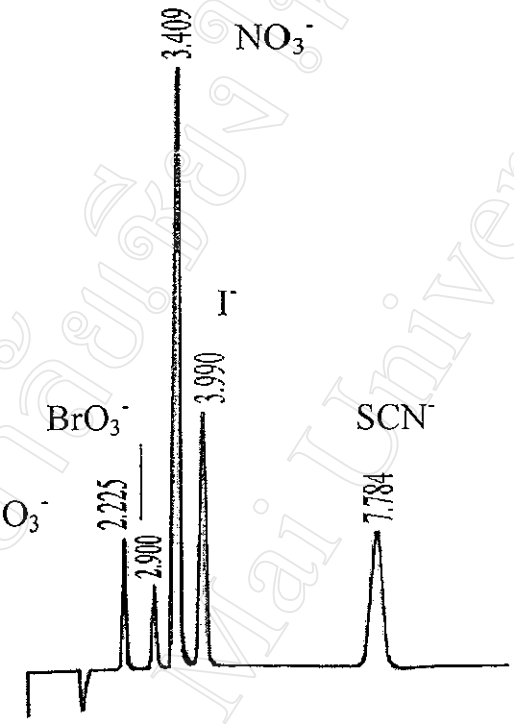

Figure 3.3 Chromatogram of anions obtained using the mobile phase of 5.0 mM heptylamine-phosphate, 5% (v/v) MeOH at pH 6.4±0.3 with a flow rate of 0.5 mL/min and 200 nm as a detection wavelength.

ลิขสิทธิ์มหาวิทยาลัยเชียงใหม่
Chiang Mai University

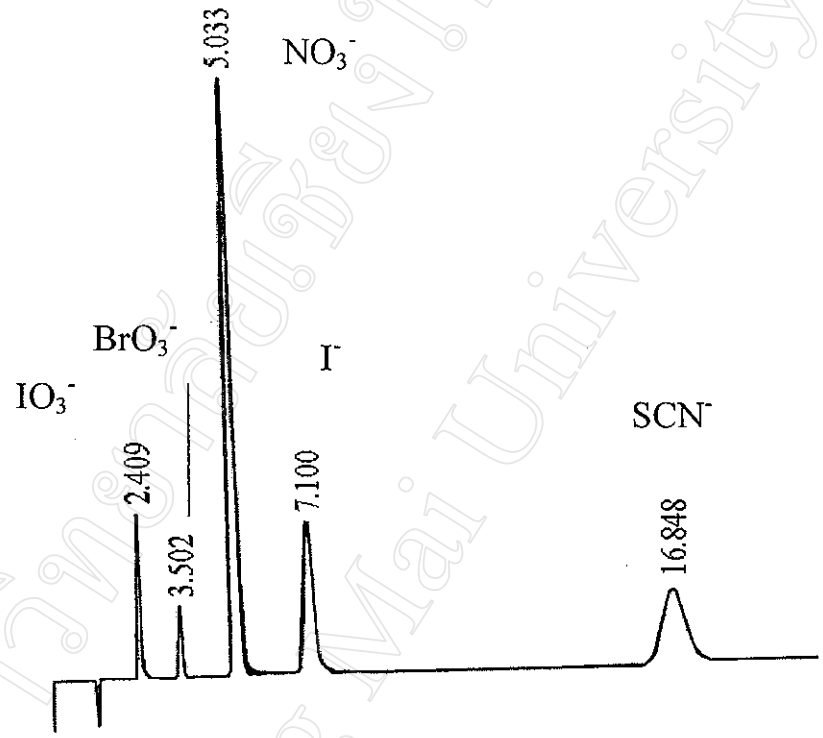

Figure 3.4 Chromatogram of anions obtained using the mobile phase of 5.0 mM octylamine-phosphate, 5% (v/v) MeOH at pH 6.4±0.3 with a flow rate of 0.5 mL/min and 200 nm as a detection wavelength.

มหาวิทยาลัยเชียงใหม่ Chiang Mai University

Table 3.2 Retention times and peak areas of each anion obtained by using three different mobile phases (n = 3)

Anion	Retention time (min) in			Peak Areas (arbitrary unit) of		
	hexylamine	heptylamine	octylamine	hexylamine	heptylamine	octylamine
IO_3^-	1.812	2.225	2.409	613310	586378	601854
BrO_3^-	2.130	2.900	3.502	416796	433824	389032
NO_3^-	2.331	3.409	5.033	4041008	3537634	4103578
I^-	2.740	3.990	7.100	1316535	1675710	1700847
SCN^-	4.647	7.784	16.848	1999447	1944866	2122429

Note : Mobile phase used : 5.0 mM alkylamine-phosphate + 5 % v/v MeOH at pH 6.4 ±0.3

Flow rate : 0.5 mL/min

Detection wavelength : 200 nm

ลิขสิทธิ์มหาวิทยาลัยเชียงใหม่
Chiang Mai University

Table 3.3 Effect of the types of ion-interaction reagent on the resolution (R_S) of some anions

Pair of anions	Resolution (R_S)		
	Hexylamine	Heptylamine	Octylamine
IO_3^-&BrO_3^-	1.360	2.214	3.143
BrO_3^-&NO_3^-	0.640	1.827	3.600
NO_3^-& I^-	0.978	1.940	3.330
I^-& SCN^-	3.382	3.833	5.692

3.1.2 Wavelength of detection

Since the sensitivity of detection depends on the wavelength of detection, in order to obtain the optimum operating conditions for chromatographic separation the wavelength of detection was investigated by varying in the range of 200-230 nm. Again the standard mixture and chromatographic conditions are the same as being used in the previous study on the types of ion interaction reagent.

Figure 3.5 shows the chromatograms of anions at various wavelengths, whereas **Figure 3.6** depicts a relationship between wavelengths of detection and peak areas of the anions. The average peak areas and the retention times of anions from triplicate runs as a function of wavelength measured at 200-230 nm are shown in **Table 3.4**.

It was found that at higher wavelength, the sensitivities of mixed standard anion were reduced, except the peak area of iodide at wavelength 210 nm increased. It was also found that at 230 nm the highest peak area for iodide was yielded, while for other anions at the wavelength of 200 nm they produced the highest peak area. Therefore throughout this work, the optimal wavelength chosen was 200 nm.

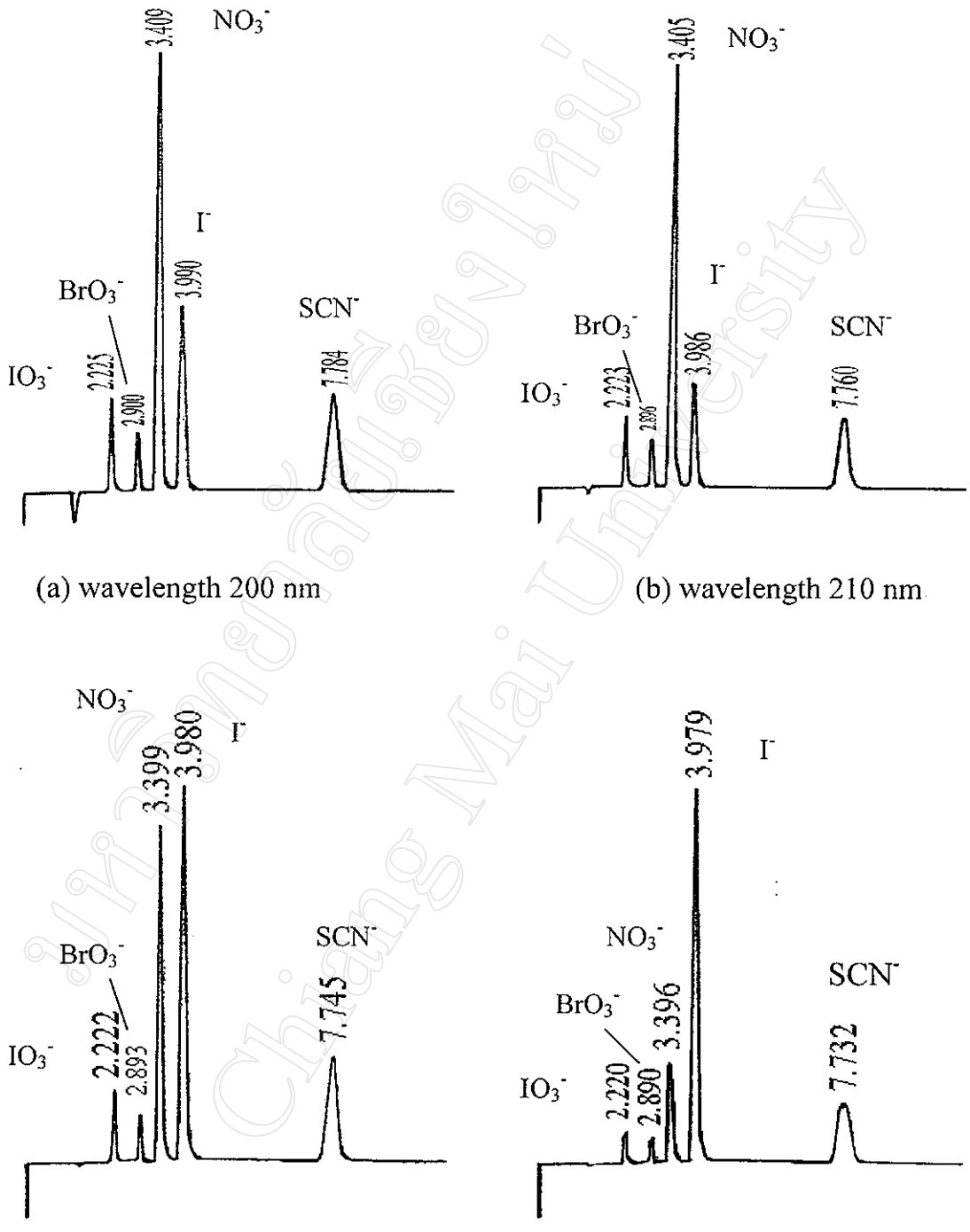

(a) wavelength 200 nm (b) wavelength 210 nm

(c) wavelength 220 nm (d) wavelength 230 nm

Figure 3.5 Chromatograms of anions illustrate the effect of detection wavelengths.

Table 3.4 Effect of wavelength of detection on peak area of each anion

Anion	Retention time (min) at				Peak Area (arbitrary unit) at			
	200 nm	210 nm	220 nm	230 nm	200 nm	210 nm	220 nm	230 nm
IO_3^-	2.225	2.223	2.222	2.220	586378	387436	233840	134930
BrO_3^-	2.900	2.896	2.893	2.890	433824	294048	187942	75834
NO_3^-	3.409	3.405	3.399	3.396	3537634	2975310	1484684	347135
I^-	3.990	3.986	3.980	3.979	1675710	808182	1845487	2103381
SCN^-	7.784	7.760	7.745	7.732	1944866	1223718	1136648	618756

ลิขสิทธิ์มหาวิทยาลัยเชียงใหม่
Chiang Mai University

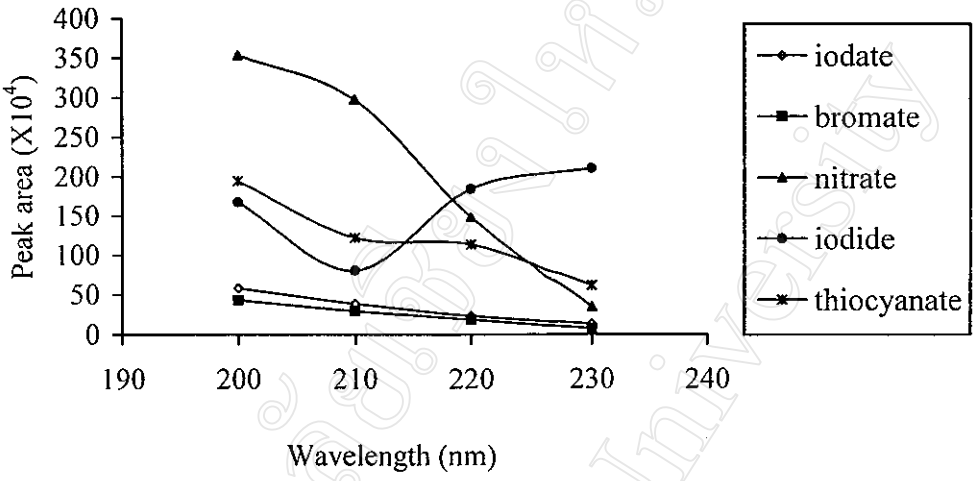

Figure 3.6 Relationship between the wavelength of detection and peak areas of each anion.

มหาวิทยาลัยเชียงใหม่ Chiang Mai University

3.1.3 The flow rate

The effect of the mobile phase flow rate on retention time, peak areas and resolution between each anion pair was studied by using the same experimental conditions as previously done in the past two parameters of which the type of ion interaction reagent and the wavelength of detection had been optimized. In this study, the flow rate was varied from 0.5 to 0.8 mL/min

Figure 3.7 shows the chromatogram of anions at different flow rates together with the accompanying retention time, peak areas and the resolution between each anion pair in **Table 3.5-3.6**. While **Figure 3.8** illustrates the relationship between the flow rate and the retention time.

The observations clearly indicate that using a low flow rate results in an increase of a retention time of anion. This happening is again obvious and can be explained in term of the partitioning abilities of the ion pairs into the nonpolar stationary phase. A slow flow rate allows the partition to occur better than a fast flow rate, thus the ion pairs can sustain longer in the stationary phase. However, the variation of flow rate in the studied range poses no negative effect on the separation. The separation of all anions at all flow rate studied are complete with high values of resolution (R_S >1.5). Therefore, the pressure drop across the column and the amount of mobile phase consumed would be the key factors for consideration in order to select an appropriate flow rate. So 0.5 mL/min was selected for further study due to a lower pressure drop of the pump system.

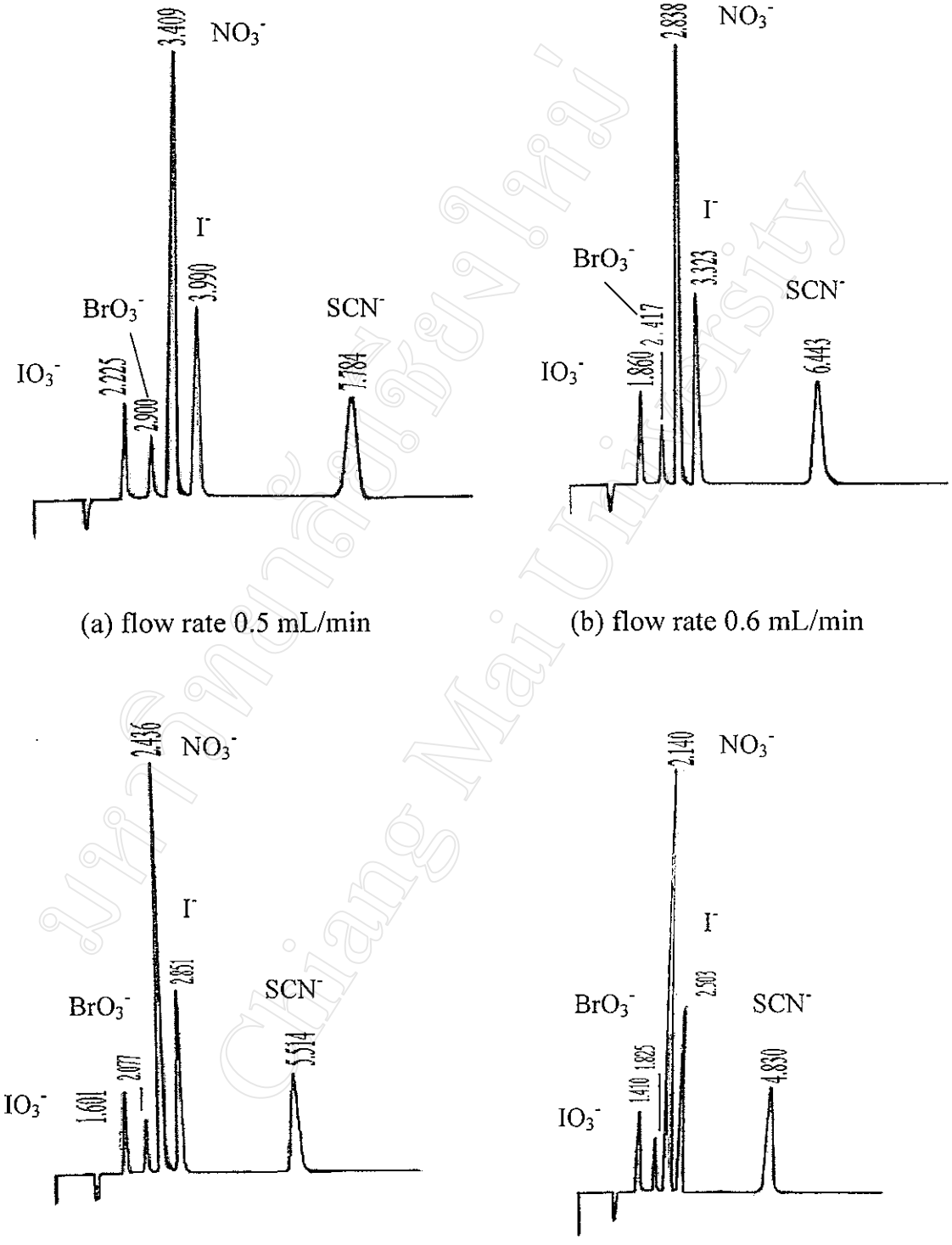

(a) flow rate 0.5 mL/min

(b) flow rate 0.6 mL/min

(c) flow rate 0.7 mL/min

(d) flow rate 0.8 mL/min

Figure 3.7 Chromatograms of anions demonstrate the effect of mobile phase flow rates.

Table 3.5 Effect of the flow rate of the mobile phase on retention time and peak area of each anion

Anion	Retention time (min) at a flow rate of				Peak Area (arbitrary unit) at a flow rate of			
	0.5 mL/min	0.6 mL/min	0.7 mL/min	0.8 mL/min	0.5 mL/min	0.6 mL/min	0.7 mL/min	0.8 mL/min
IO_3^-	2.225	1.860	1.601	1.410	586378	512491	431138	389290
BrO_3^-	2.900	2.417	2.077	1.825	433824	384021	316703	285844
NO_3^-	3.409	2.838	2.436	2.140	3537634	3081528	2599510	2326350
I^-	3.990	3.323	2.851	2.503	1675710	1501775	1266346	1134919
SCN^-	7.784	6.443	5.514	4.830	1944866	1702366	1437626	1290317

Table 3.6 Resolution (R_S) of each anion pair at various flow rates

Anions pair	Resolution (R_S) of each anion pair at a flow rate of			
	0.5 mL/min	0.6 mL/min	0.7 mL/min	0.8 mL/min
IO_3^-&BrO_3^-	2.214	2.198	2.006	1.876
BrO_3^-&NO_3^-	1.827	1.686	1.605	1.523
NO_3^-& I^-	1.940	1.728	1.580	1.545
I^-& SCN^-	3.833	3.790	3.714	3.674

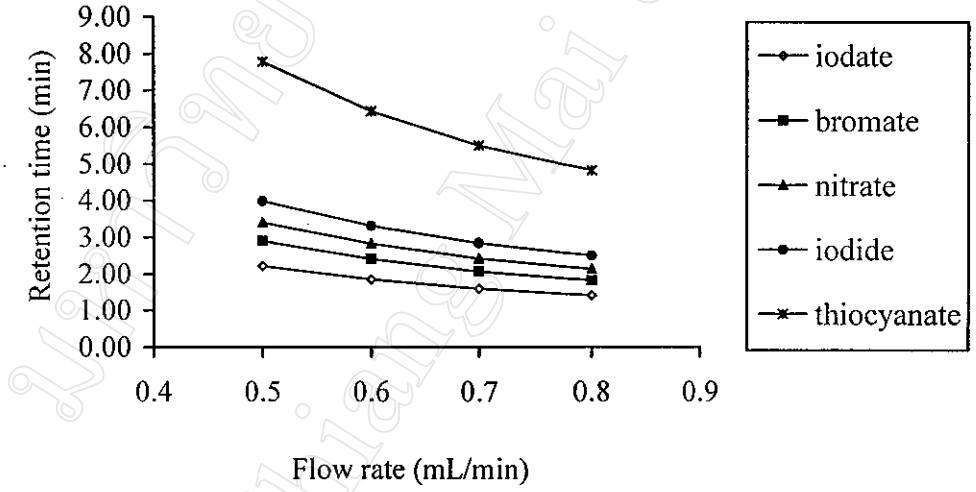

Figure 3.8 Relationship between the flow rate of the mobile phase and the retention time of each anion.

3.1.4 The concentration of ion interaction reagent

From the experiment, it was found that the retention time of anions tended to increase when the concentration of heptylamine increased, but at a concentration higher than 10.0 mM, the retention time of most ions seemed to be relatively constant. This can be explained through a greater functionalization of the stationary phase induced by a more concentrated eluent. The anion of the salt seems to compete with the solute for the active site on the stationary phase or to exert an electrostatic shielding, that affects not only retention (which generally decreases with the increase in ionic strength) but also the selectivity and the elution order [48]. Usually, the concentration of ion interaction reagent should be used in the range of 5.0-10.0 mM. The increase in the concentration of ion interaction reagent will limit the retention to a certain level which affects the equilibrium attaining the ion pair formation. However, if the concentration becomes too high, it will result in the decrease of the retention [14]. Therefore, at concentration of 5 mM heptylamine-phosphate was found to be optimum in this works because it offerred acceptable analysis time and resolution of anion pair and it also consumed less amount of used little ion interaction reagent.

Once the parameters of type of ion interaction reagent, wavelength of detection and the flow rate were optimized, they were used in setting the condition for finding out the appropriate concentration of the ion interaction reagent. Again all chromatographic conditions were set as usual except the concentration of the ion interaction reagent was varied in the range of 5.0-20.0 mM by 5.0 mM increment.

This time, the dependence of the retention times, peak areas and the resolution of each anion pair on the concentration of heptylamine-phosphate (the ion interaction reagent) are illustrated in **Figure 3.9** and **Tables 3.7-3.8**. In a similar fashion, the relationship between the concentrations of the ion interaction reagent and the retention time is shown graphically in **Figure 3.10**.

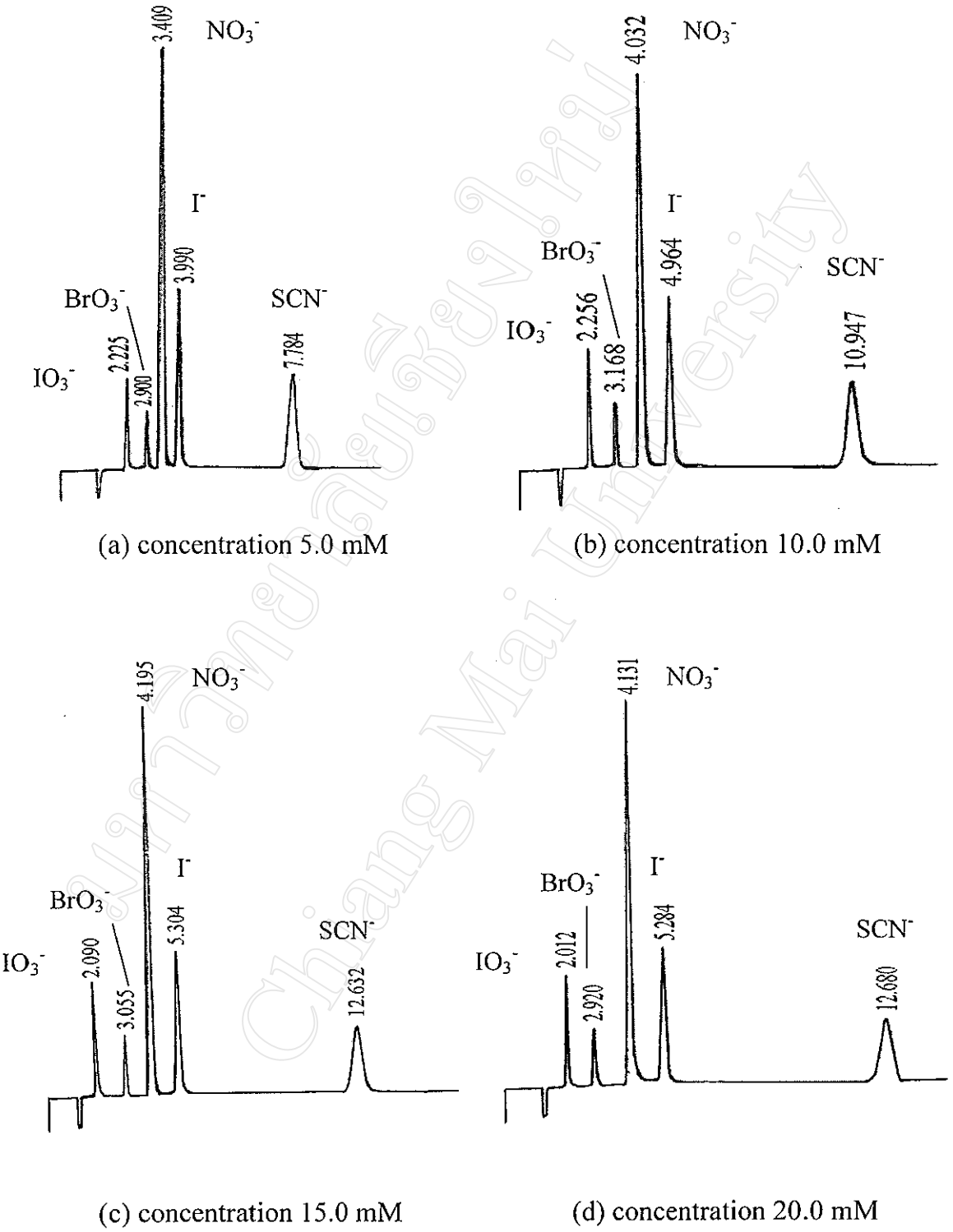

(a) concentration 5.0 mM (b) concentration 10.0 mM

(c) concentration 15.0 mM (d) concentration 20.0 mM

Figure 3.9 Chromatograms illustrate the effect of concentration of heptylamine on anions separation.

ลิขสิทธิ์มหาวิทยาลัยเชียงใหม่
Chiang Mai University

Table 3.7 Effect of the ion interaction reagent concentration on retention time and peak area of each anion

Anion	Retention time (min) in heptylamine at a concentration of				Peak Area (arbitrary unit) in heptylamine at a concentration of			
	5 mM	10 mM	15 mM	20 mM	5 mM	10 mM	15 mM	20 mM
IO_3^-	2.225	2.256	2.090	2.012	586378	561160	602078	623256
BrO_3^-	2.900	3.168	3.055	2.920	433824	392177	371006	389116
NO_3^-	3.409	4.032	4.195	4.131	3537634	3602158	3653805	4037261
I^-	3.990	4.964	5.304	5.284	1675710	1604493	1680004	1718691
SCN^-	7.784	10.947	12.632	12.680	1944866	1853039	2003311	2532933

ลิขสิทธิ์มหาวิทยาลัยเชียงใหม่
Chiang Mai University

Table 3.8 Resolution (R_S) of each anion pair at various the concentrations of ion interaction reagent

Anions pair	Resolution (R_S) of each anion pair at heptylamine concentration of			
	5 mM	10 mM	15 mM	20 mM
IO_3^-&BrO_3^-	2.214	2.987	2.766	2.542
BrO_3^-&NO_3^-	1.827	2.260	2.565	2.564
NO_3^-& I^-	1.940	2.223	2.349	2.440
I^-& SCN^-	3.833	6.737	7.014	6.964

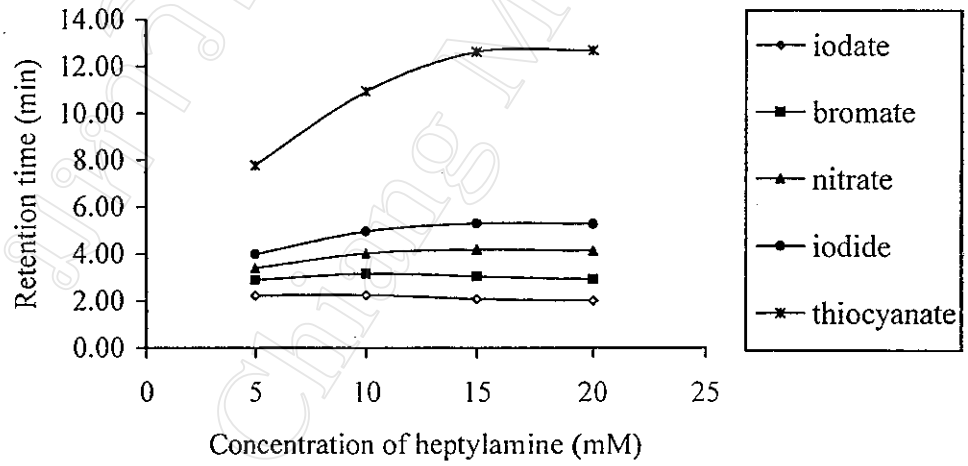

Figure 3.10 Relationship between the concentration of ion interaction reagent and the retention time of each anion.

3.1.5 pH

The pH is another factor that needed to be optimized for anion separation. By following the same train of optimization procedure that each optimized parameter is fixed after each optimization, this optimization step was carried out by using the conditions as follows: 5.0 mM heptylamine–phosphate (+5 % v/v MeOH) was used as a mobile phase at a flow rate of 0.5 mL/min, together with the detection was done at 200 nm. The volume of injection was 20 μL throughout the experiment and the pH was varied from 4.4-7.4.

The results from the experiment are visualized in the same manner as previously done for other parameters in **Figure 3.11** and **Table 3.9-3.10** as well as **Figure 3.12** that shows the relationship between the retention time with the studied parameters.

It is not surprised that the retention time of anions continuously decreased with the increase in pH of the mobile phase. The role of the pH of mobile phase will play on the availability of the active sites on the stationary phase that occur from the partition of the hydrophobic and of the cationic form to form the primary electrical layer. The decrease of the pH will adversely affect the amount of phosphate counter ion present in the mobile phase. This phosphate ion competes with the investigated anions to from a secondary layer. Thus, at a higher pH, more phosphate ions are available and occupy most of the active sites. Therefore the retention times of the investigated anions tend to decrease with the increase of the pH of the mobile. However it was observed that the pH of the mobile phase had a pronounced effect on the retention of the thiocyanate ion.

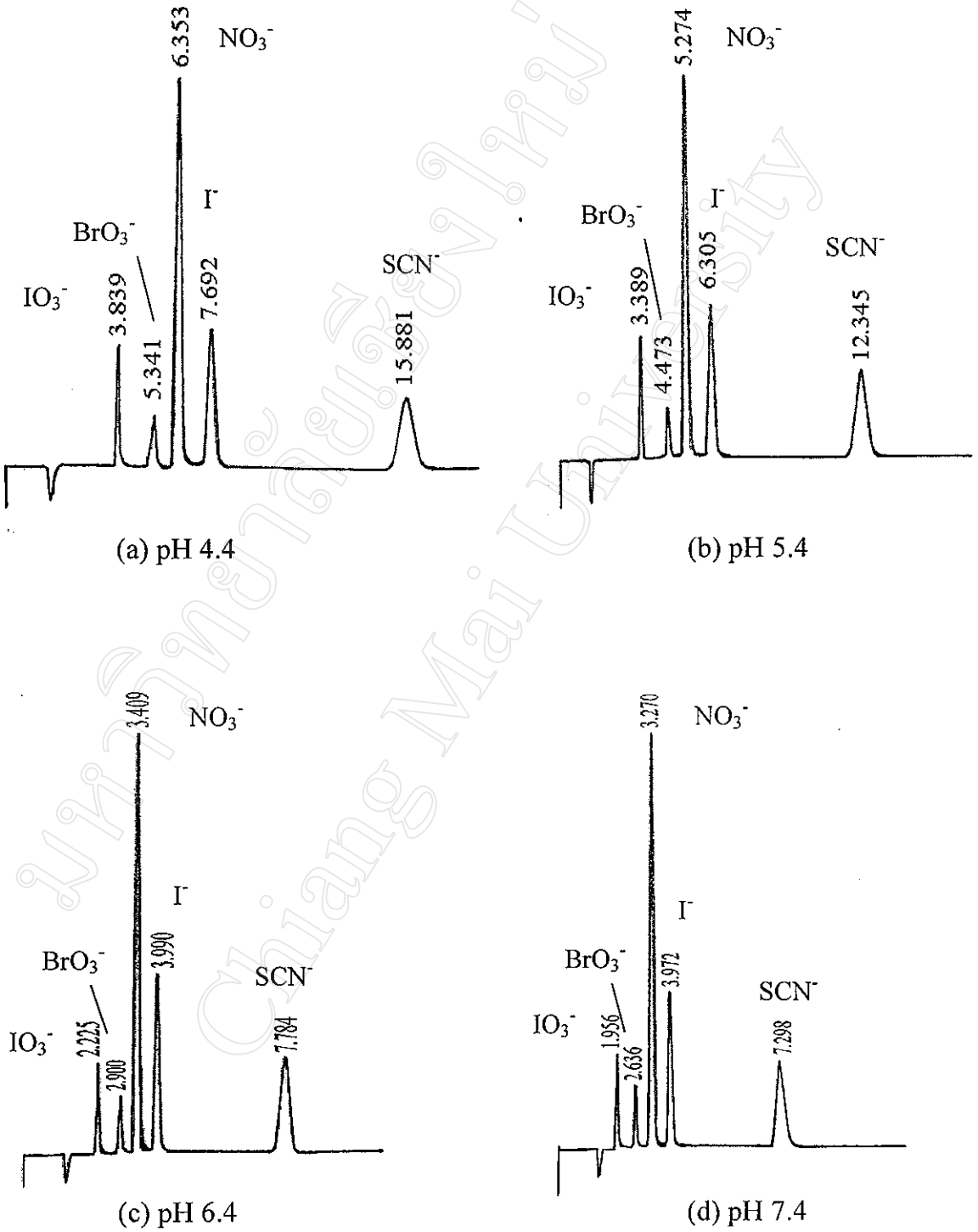

Figure 3.11 Chromatograms reveal the effect of pH on anions separation.

Table 3.9 Effect of the pH of the mobile phase on retention time and peak area of each anion

Anion	Retention time (min) at				Peak Area (arbitrary unit)			
	pH 4.4	pH 5.4	pH 6.4	pH 7.4	pH 4.4	pH 5.4	pH 6.4	pH 7.4
IO_3^-	3.839	3.389	2.225	1.956	619484	518203	586378	580141
BrO_3^-	5.341	4.473	2.900	2.636	394837	596973	433824	461438
NO_3^-	6.353	5.274	3.409	3.270	3654186	3316038	3537634	3785021
I^-	7.692	6.305	3.990	3.972	1641114	1605463	1675710	1708273
SCN^-	15.881	12.345	7.784	7.298	2030225	1889621	1944866	2251682

Table 3.10 Resolution (R_S) of each anion pair at various pH

Anions pair	Resolution (R_S) of each anion pair at			
	pH 4.4	pH 5.4	pH 6.4	pH 7.4
IO_3^-&BrO_3^-	3.845	3.335	2.214	2.200
BrO_3^-&NO_3^-	2.892	2.296	1.827	1.803
NO_3^-& I^-	3.136	2.828	1.940	1.786
I^-& SCN^-	6.484	5.955	3.833	3.684

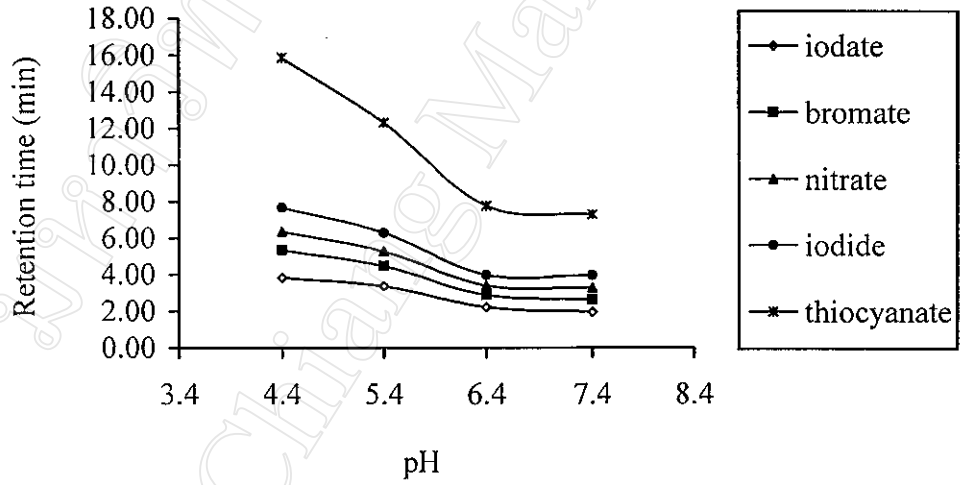

Figure 3.12 Relationship between pH and the retention time of each anion.

3.1.6 The concentration of organic modifier

The last parameter investigated was the effect of the organic modifier concentration importing on the separation of anions. All parameters previously studied were fixed at the appropriate values in this fashion; mobile phase: 5.0 mM heptylamine-phosphate (plus various amounts of MeOH) at pH 6.4±0.3; flow rate: 0.5 mL/min; detection wavelength: 200 nm and injection volume: 20 µL. The amount of methanol functional as an organic modifier was varied in the concentration range of 0-15 % v/v.

Figure 3.13 and **Table 3.11-3.12** display the variation of the retention time, peak area and the resolution of each anion pair upon the change of the methanol concentration, whereas **Figure 3.14** reveals the change of retention time of each anion as a function of methanol concentration.

The results appear as when the concentration of organic modifier increases the retention times of the anion decrease. At 0 % (v/v) MeOH has longest retention time and at 15 % MeOH has resolution not good. The effect of the organic modifier contained in the mobile phase, it was shown that, as expected, retention decreases when the concentration of the organic modifier increases. This effect is due to (besides the increased eluotropic strength of the solvent) desorption effects exerted by the organic solvent toward the moiety adsorbed on to the surface and to competition equilibria taking place between the solvent and the modifier. The adjustment of organic modifier concentration in the mobile phase can therefore regulate the amount of the ion interaction reagent adsorbed and by consequence the retention [49-51].

Resolutions and retention times of all anions were practically acceptable for both concentrations, but the concentration of 5 % v/v was chosen as the optimum concentration due to a better resolution and an acceptable analysis time (<10 min). Another reason that 10 % v/v methanol was not chosen because baseline drifts were sometimes observed as well as the shift of the eluted peaks that caused the overlapping at this concentration.

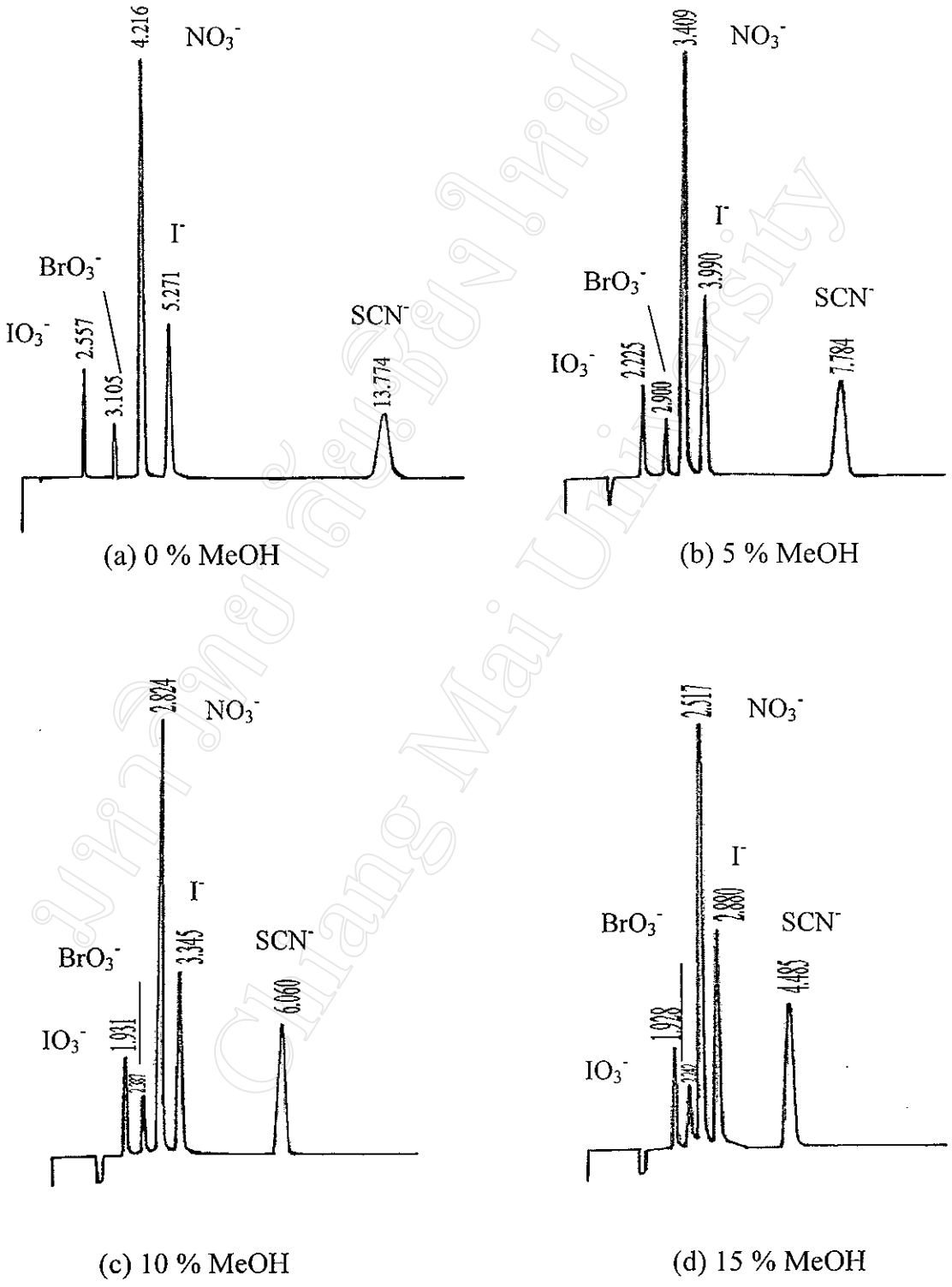

Figure 3.13 Chromatograms of anions reveal the effect of % MeOH on the separation.

Table 3.11 Effect of the organic modifier concentration on retention time and peak area of each anion

Anion	Retention time (min) in				Peak Area (arbitrary unit)			
	0 % MeOH	5 % MeOH	10 % MeOH	15 % MeOH	0 % MeOH	5 % MeOH	10 % MeOH	15 % MeOH
IO_3^-	2.557	2.225	1.931	1.928	594387	586378	579377	579377
BrO_3^-	3.105	2.900	2.387	2.242	435400	433824	432202	432202
NO_3^-	4.216	3.409	2.824	2.517	3551186	3537634	3526336	3526336
I^-	5.271	3.990	3.345	2.880	1647251	1675710	1513050	1513050
SCN^-	13.774	7.784	6.060	4.485	2051144	1944866	2176270	2176270

ลิขสิทธิ์มหาวิทยาลัยเชียงใหม่
Chiang Mai University

Table 3.12 Resolution (R_S) of each anion pair at various the concentrations of organic modifier

Anions pair	Resolution (R_S) of each anion pair in			
	0% MeOH	5% MeOH	10% MeOH	15% MeOH
IO_3^-&BrO_3^-	3.706	2.214	1.875	1.556
BrO_3^-&NO_3^-	2.845	1.827	1.436	0.748
NO_3^-& I^-	2.563	1.940	1.475	1.080
I^-& SCN^-	8.286	3.833	3.542	3.934

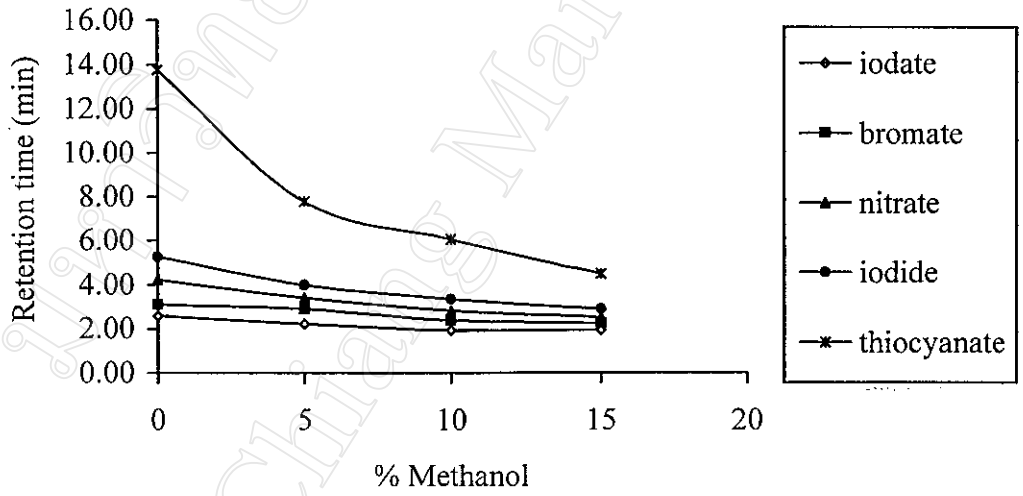

Figure 3.14 Relationship between the concentration of organic modifier and the retention time of each anion.

3.1.7 Summary of the optimized HPLC conditions

The optimized HPLC conditions established in this work is summarized in **Table 3.13** and this condition was used throughout this work.

Table 3.13 Summary of the optimized HPLC conditions

Operation	Optimal Condition
Stationary phase	C_{18} reversed-phase
Mobile phase	5.0 mM Heptylamine-phosphate, pH 6.4±0.3 with 5% MeOH (v/v)
Flow rate	0.5 mL/min
Wavelength	200 nm
Injection volume	20 μL

ลิขสิทธิ์มหาวิทยาลัยเชียงใหม่ Chiang Mai University

3.2 Characteristics of the analysis

Several characteristics of the procedure were checked in order to ensure the proper operation of the column and the chromatograph. These characteristics include the linearity range, the reproducibility of the method, detection limit and percent recovery. This was done by using the same chromatographic conditions which consisted of 5.0 mM heptylamine-phosphate at pH 6.4±0.3 together with 5 % v/v MeOH as the mobile phase. The flow rate was adjusted to be 0.5 mL/min and the separating column used was Microsorb MV-100, 3 μm C-18 (4.6 x 50 mm.) with the detection at 200 nm.

3.2.1 Linearity range

When 20 μL of standard mixture each of IO_3^-, BrO_3^-, NO_3^-, I^- and SCN^- ranging from 0.04-100 ppm were injected into the chromatographic system. The result obtained is shown in **Table 3.14** and their graphic representations which depict the relationship between peak area with concentration in the range of 0.04-100 ppm of each anion are shown in **Figure 3.15-3.19**.

Under these chromatographic conditions for analysis of some anions, the calibration curves show very good dynamic range of detection from 0.04 to 100 ppm with excellent linear response. The linearity ranges of anion given in **Table 3.15** are seen to cover the narrow concentration range of 0.04-100 ppm, because the analytical column used in this work could not tolerate a higher loading as it has been used for quite some time. These results are based on triplicate runs which provide reliable data for implementing the procedure for the analysis of such anions.

Table 3.14 Relationship between peak areas and the concentrations of anions

Concentration (ppm)	Peak area ($1x10^4$) (arbitrary unit)				
	Iodate	Bromate	Nitrate	Iodide	Thiocyanate
0.04	0.582	0.443	11.320	5.369	2.046
0.06	0.610	0.676	13.864	7.772	2.285
0.08	0.910	0.776	15.568	9.236	3.924
0.10	1.067	1.180	17.282	10.509	5.742
0.20	1.563	1.645	22.675	16.889	8.842
0.40	3.124	2.679	34.693	25.323	17.816
0.60	4.725	4.036	46.064	37.113	26.940
0.80	6.522	5.346	54.840	49.359	33.693
1.00	10.006	6.006	71.888	56.267	40.554
2.00	10.726	12.061	127.475	84.927	77.215
3.00	20.227	20.417	208.015	124.812	127.215
4.00	32.905	29.216	282.451	153.032	177.016
5.00	58.775	37.341	346.404	183.674	215.724
10.00	112.524	72.147	690.274	352.550	425.508
20.00	242.718	142.602	1361.681	691.513	846.755
40.00	436.558	273.401	2808.915	1376.321	1695.138
60.00	668.836	420.748	4283.078	2127.552	2558.595
80.00	889.356	567.729	5766.679	2841.808	3454.934
100.00	1094.894	685.193	6855.270	3472.339	4237.562

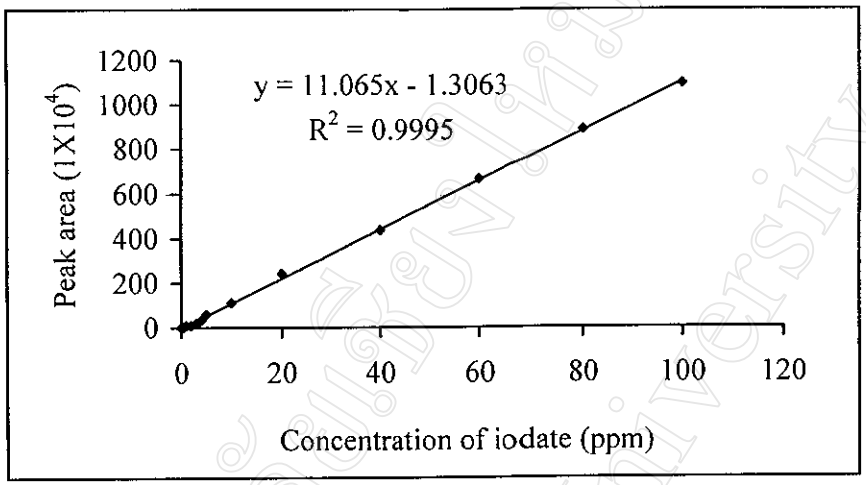

Figure 3.15 Linearity of iodate in the range 0.04-100 ppm.

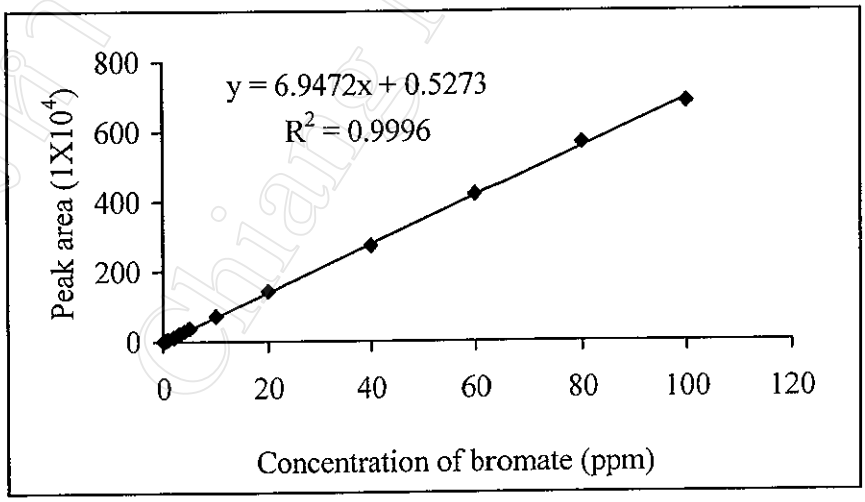

Figure 3.16 Linearity of bromate in the range 0.06-100 ppm.

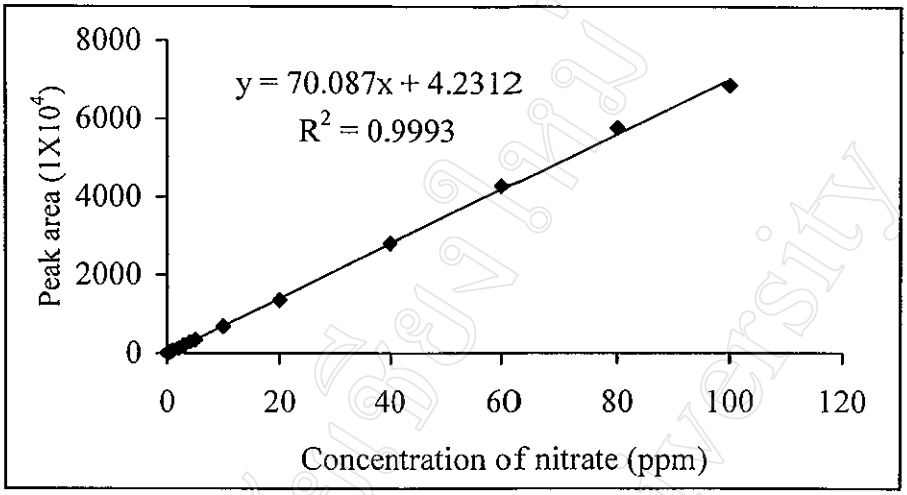

Figure 3.17 Linearity of nitrate in the range 0.06-100 ppm.

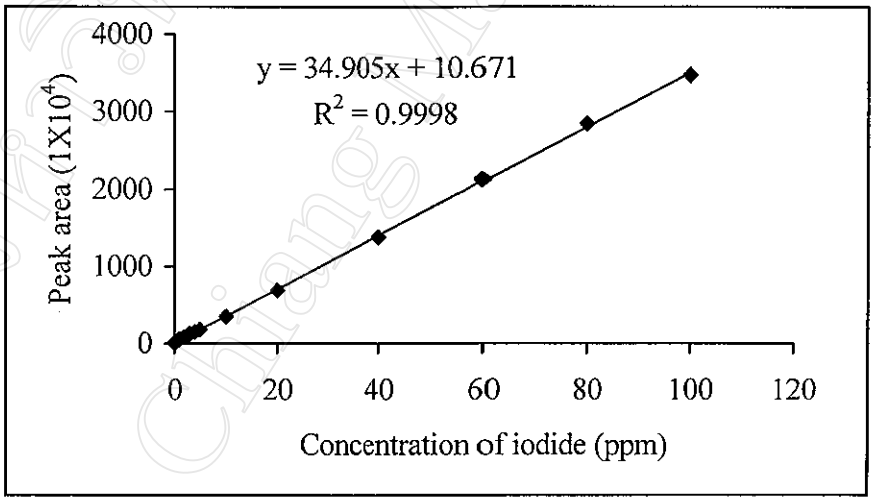

Figure 3.18 Linearity of iodide in the range 0.06-100 ppm.

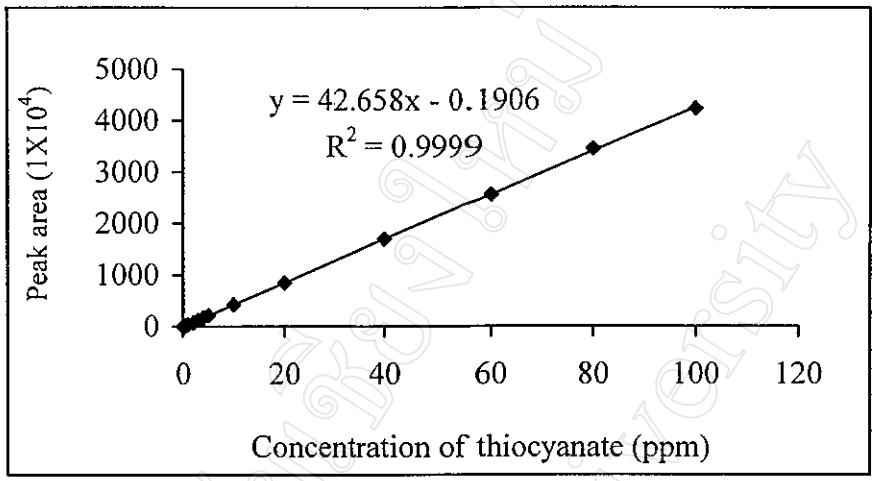

Figure 3.19 Linearity of thiocyanate in the range 0.04-100 ppm.

Table 3.15 Summary of linearity range of each anion

Anion	Correlation coefficient (R^2)	Linearity range (ppm)
Iodate	Y = 11.065x -1.3063 R^2 = 0.9995	0.04-100
Bromate	Y = 6.9472x + 0.5273 R^2 = 0.9996	0.06-100
Nitrate	Y = 70.087x + 4.2312 R^2 = 0.9993	0.06-100
Iodide	Y = 34.905x + 10.671 R^2 = 0.9998	0.06-100
Thiocyanate	Y = 42.658x – 0.1906 R^2 = 0.9999	0.04-100

3.2.2 Reproducibility of results

The reproducibilities of the retention time and the peak area was studied by five replicate injections of 20 μL of a mixed standard into the chromatographic system under the above conditions by varying attenuation of detector to be 32, 64 and 128, respectively. The results obtained is shown in **Table 3.16-3.20**.

Table 3.16 Relationship between t_R and peak area of iodate at various attenuations

No.	Attenuation					
	32		64		128	
	t_R (min)	Peak area ($x10^4$)	t_R (min)	Peak area ($x10^4$)	t_R (min)	Peak area ($x10^4$)
1	2.223	55.370	2.237	56.410	2.229	56.420
2	2.231	53.240	2.236	56.000	2.222	56.480
3	2.230	55.060	2.236	56.500	2.225	55.740
4	2.230	55.500	2.234	53.920	2.224	55.530
5	2.230	56.480	2.232	55.130	2.222	55.630
Mean	2.231	55.130	2.235	55.600	2.224	55.970
S.D.	$1.323x10^{-3}$	$1.180 x10^{-1}$	$2.000x10^{-3}$	$1.080 x10^{-1}$	$2.915x10^{-3}$	$4.400 x10^{-2}$
% R.S.D	0.059	2.140	0.089	1.942	0.131	0.786

Table 3.17 Relationship between t_R and peak area of bromate at various attenuations

No.	Attenuation					
	32		64		128	
	t_R (min)	Peak area ($x10^4$)	t_R (min)	Peak area ($x10^4$)	t_R (min)	Peak area ($x10^4$)
1	2.823	40.490	2.829	40.100	2.819	39.780
2	2.822	40.260	2.828	39.120	2.810	40.480
3	2.820	41.310	2.826	38.880	2.815	41.330
4	2.820	41.120	2.824	38.880	2.813	40.270
5	2.819	41.100	2.822	39.540	2.811	39.980
Mean	2.821	40.860	3.930	39.300	2.814	40.370
S.D.	$1.658x10^{-3}$	$4.500 x10^{-2}$	$2.872x10^{-3}$	$5.200 x10^{-2}$	$3.606x10^{-3}$	$6.000 x10^{-2}$
% R.S.D	0.059	1.101	0.102	1.323	0.128	1.486

Table 3.18 Relationship between t_R and peak area of nitrate at various attenuations

No.	Attenuation					
	32		64		128	
	t_R (min)	Peak area ($x10^4$)	t_R (min)	Peak area ($x10^4$)	t_R (min)	Peak area ($x10^4$)
1	3.360	369.540	3.365	377.020	3..357	375.970
2	3.359	364.720	3.365	373.760	3.350	375.880
3	3.359	368.960	3.361	378.740	3.356	374.820
4	3.358	377.700	3.359	358.800	3.354	370.760
5	3.357	378.230	3.358	366.030	3.352	372.170
Mean	3.359	371.830	3.362	370.870	3.354	373.920
S.D.	$1.225x10^{-3}$	$6.960\ x10^{-1}$	$3.317x10^{-3}$	$8.230\ x10^{-1}$	$1.436x10^{-3}$	$2.340\ x10^{-1}$
% R.S.D	0.365	1.872	0.099	2.243	0.043	0.626

มหาวิทยาลัยเชียงใหม่ Chiang Mai University

Table 3.19 Relationship between t_R and peak area of iodide at various attenuations

No.	Attenuation					
	32		64		128	
	t_R (min)	Peak area ($x10^4$)	t_R (min)	Peak area ($x10^4$)	t_R (min)	Peak area ($x10^4$)
1	4.192	189.000	4.198	197.450	4.191	194.840
2	4.193	187.310	4.199	193.470	4.187	195.830
3	4.194	191.650	4.195	195.720	4.195	197.280
4	4.194	197.360	4.190	182.660	4.191	194.130
5	4.191	197.070	4.190	187.670	4.189	193.620
Mean	4.193	192.480	4.194	191.390	4.191	195.140
S.D.	$1.225x10^{-3}$	$4.590\ x10^{-1}$	$4.301x10^{-3}$	$6.120\ x10^{-1}$	$3.000x10^{-3}$	$1.450\ x10^{-1}$
% R.S.D	0.029	2.385	0.102	3.198	0.072	0.743

ลิขสิทธิ์มหาวิทยาลัยเชียงใหม่
Chiang Mai University

Table 3.20 Relationship between t_R and peak area of thiocyanate at various attenuations

No.	Attenuation					
	32		64		128	
	t_R (min)	Peak area ($x10^4$)	t_R (min)	Peak area ($x10^4$)	t_R (min)	Peak area ($x10^4$)
1	7.800	204.420	7.804	207.860	7.820	209.260
2	7.811	200.110	7.807	207.000	7.835	206.730
3	7.822	202.130	7.795	205.670	7.849	204.550
4	7.819	207.660	7.886	196.780	7.840	202.860
5	7.816	210.300	7.792	200.970	7.835	205.300
Mean	7.814	204.920	7.970	203.360	7.836	205.740
S.D.	$8.631x10^{-3}$	$4.110 x10^{-1}$	$8.646x10^{-3}$	$4.670 x10^{-1}$	$1.000 x10^{-2}$	$2.410 x10^{-1}$
% R.S.D	0.110	2.006	0.111	2.293	0.128	1.171

The reproducibilities of the retention times and peak areas were calculated by performing five replicate injections. Precision may be defined as the concordance of a series of measurements of the same quantity. The results are given in **Table 3.16-3.20**. It can be seen that the relative standard deviations (% R.S.D.) of the retention times of each anion are between 0.029–0.365 % and those of peak area are between 0.626–3.198 %. Although at various attenuations, the relative standard deviation trend was not uncertain, these small values of the relative standard deviation (with 5 %) indicate that the precision of analysis is high.

3.2.3 The detection limit

The detection limit values of the present method for each anion under above conditions calculated from the external calibration curve for the concentration range of 0.04-0.8 ppm with a correlation are shown **Figure 3.20-3.24** and **Table 3.21**. (For a detailed calculation, see Appendix)

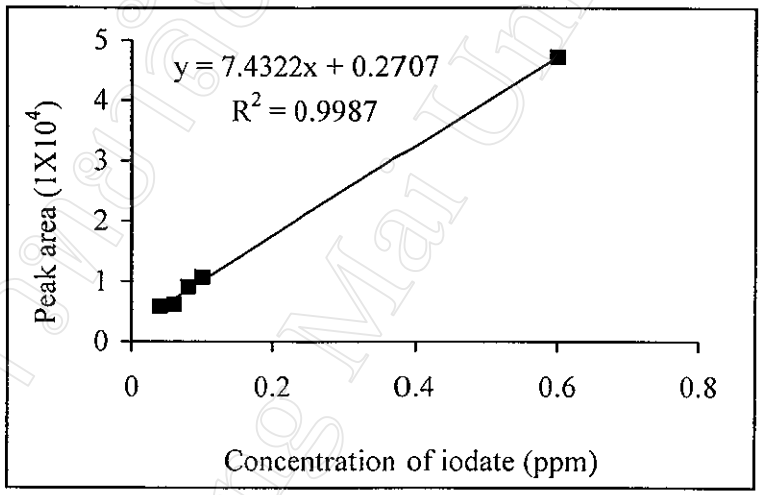

Figure 3.20 Calibration curve of iodate in the range 0.04-0.6 ppm used for calculating the detection limit.

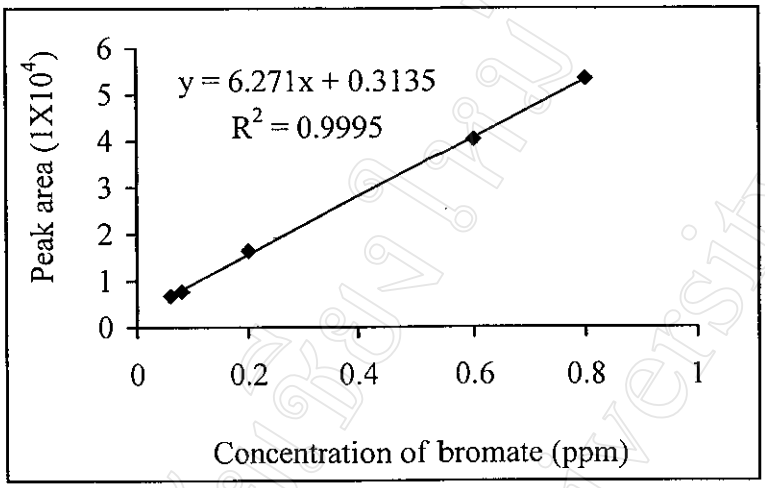

Figure 3.21 Calibration curve of bromate in the range 0.06-0.8 ppm used for calculating the detection limit.

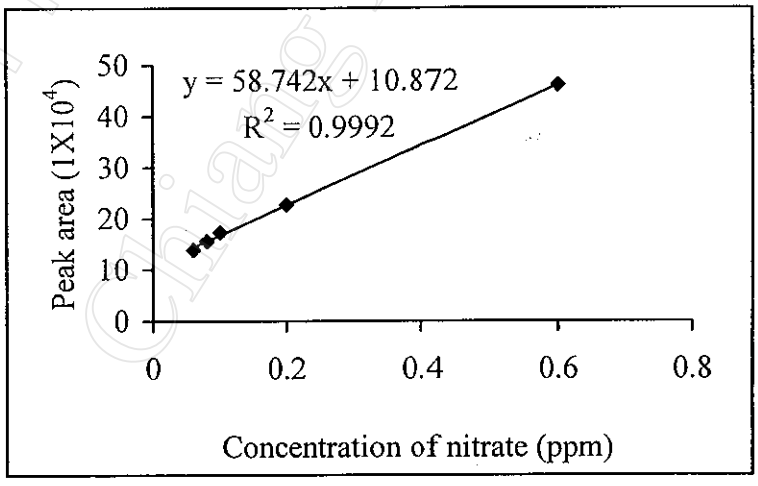

Figure 3.22 Calibration curve of nitrate in the range 0.06-0.6 ppm used for calculating the detection limit.

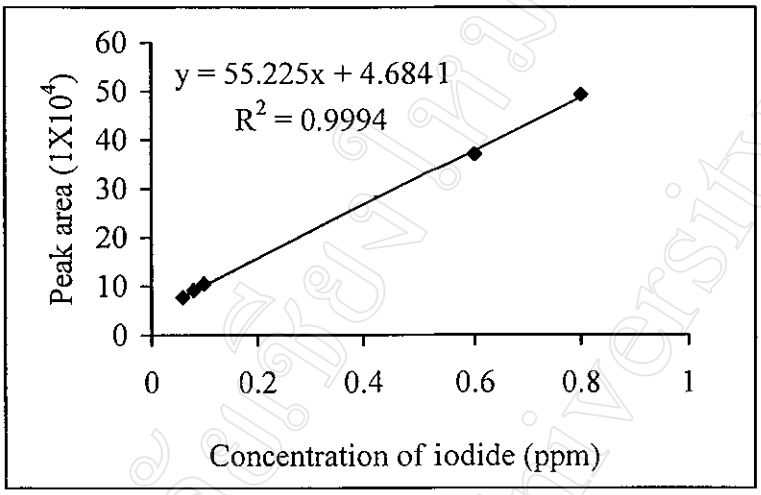

Figure 3.23 Calibration curve of iodide in the range 0.06-0.8 ppm used for calculating the detection limit.

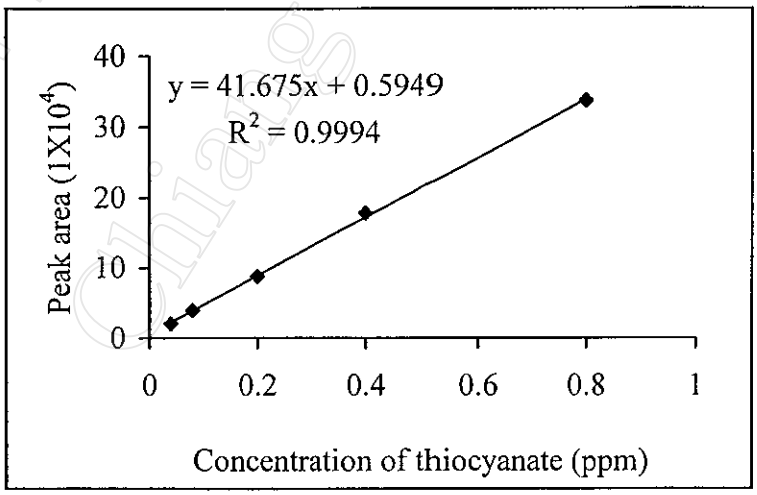

Figure 3.24 Calibration curve of thiocyanate in the range 0.04-0.8 ppm used for calculating the detection limit.

Table 3.21 Summary of detection limit of each anion

Anion	Correlation coefficient (R^2)	Detection limit (ppm)
Iodate	$Y = 7.4322x + 0.2707$ $R^2 = 0.9987$	0.031
Bromate	$Y = 6.271x + 0.3135$ $R^2 = 0.9995$	0.027
Nitrate	$Y = 58.742x + 10.872$ $R^2 = 0.9992$	0.022
Iodide	$Y = 55.225x + 4.6841$ $R^2 = 0.9994$	0.030
Thiocyanate	$Y = 41.675x + 0.5949$ $R^2 = 0.9994$	0.027

ลิขสิทธิ์มหาวิทยาลัยเชียงใหม่
Chiang Mai University

3.2.4 Percent recovery

Percent recovery of anions was again checked to verify whether the procedure and conditions used were compatible to the instrument. By preparing tap water sample containing various amounts of anions (0, 1, 2, 3, 4 ppm), 20 μL of the prepared solution were injected into the LC system. Data obtained from the chromatograms were used in conjunction with the standard curve in **Figure 3.25-3.29** and to calculate the percent recovery of each anion as presented in **Table 3.22-3.26.**

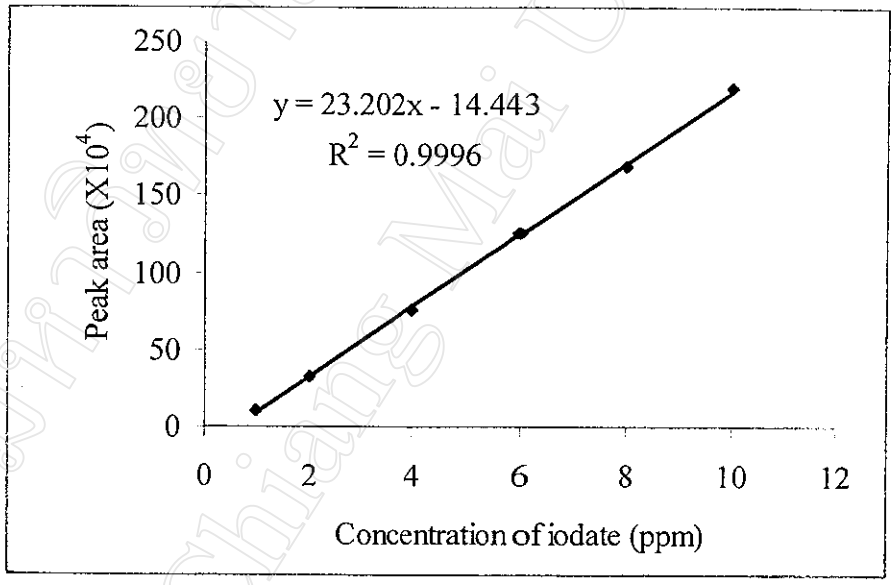

Figure 3.25 Calibration curve of iodate in water sample used for calculating % recovery.

Table 3.22 % Recovery of IO_3^- in water sample when spiked with standard IO_3^- at various concentrations

Spiked standard IO_3^- (ppm)	Peak area ($x10^4$) (arbitrary unit)	Concentration (ppm)	% Recovery
0.00	0	0	-
1.00	8.924	0.98	98.0
2.00	32.424	2.02	101.0
3.00	54.465	2.97	99.0
4.00	79.291	4.04	101.1
Average			99.8

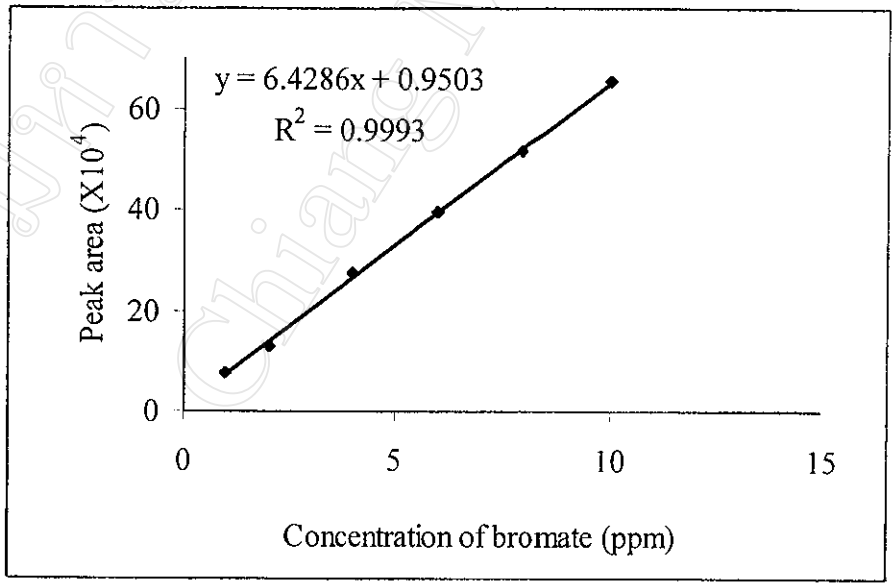

Figure 3.26 Calibration curve of bromate in water sample used for calculating % recovery.

Table 3.23 % Recovery of BrO_3^- in water sample when spiked with standard BrO_3^- at various concentrations

Spiked standard BrO_3^- (ppm)	Peak area ($x10^4$) (arbitrary unit)	Concentration (ppm)	% Recovery
0.00	0	0	-
1.00	7.443	1.01	101.0
2.00	13.550	1.96	98.0
3.00	19.529	2.89	96.0
4.00	26.279	3.94	98.5
Average			98.4

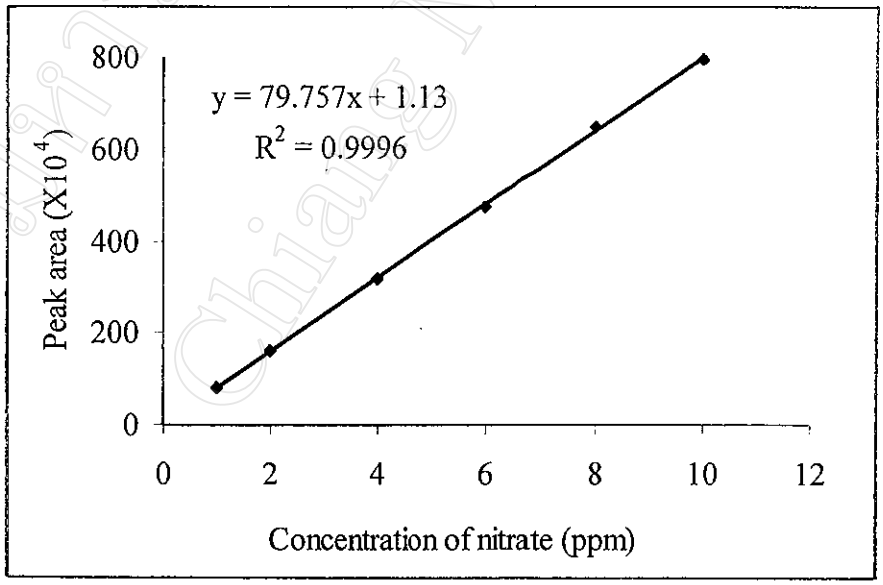

Figure 3.27 Calibration curve of nitrate in water sample used for calculating % recovery.

Table 3.24 % Recovery of NO_3^- in water sample when spiked with standard NO_3^- at various concentrations

Spiked standard NO_3^- (ppm)	Peak area ($x10^4$) (arbitrary unit)	Concentration (ppm)	% Recovery
0.00	220.696	2.75	-
1.00	297.029	3.71	96.0
2.00	375.191	4.69	97.0
3.00	455.746	5.70	98.3
4.00	526.147	6.58	95.7
Average			96.8

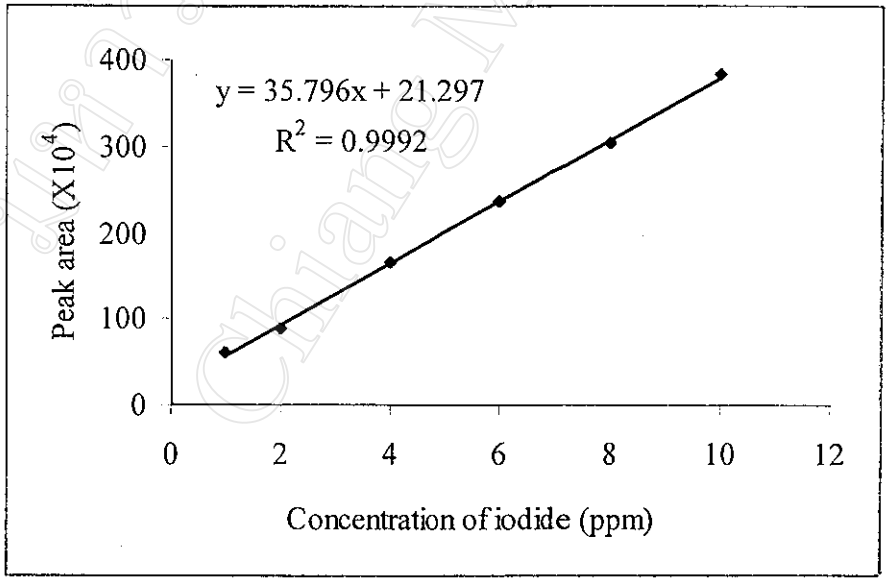

Figure 3.28 Calibration curve of iodide in water sample used for calculating % recovery.

Table 3.25 % Recovery of I^- in water sample when spiked with standard I^- at various concentrations

Spiked standard I^- (ppm)	Peak area ($x10^4$) (arbitrary unit)	Concentration (ppm)	% Recovery
0.00	0	0	-
1.00	55.661	0.96	96.0
2.00	91.815	1.97	98.5
3.00	127.252	2.96	98.7
4.00	162.690	3.95	98.8
Average			98.0

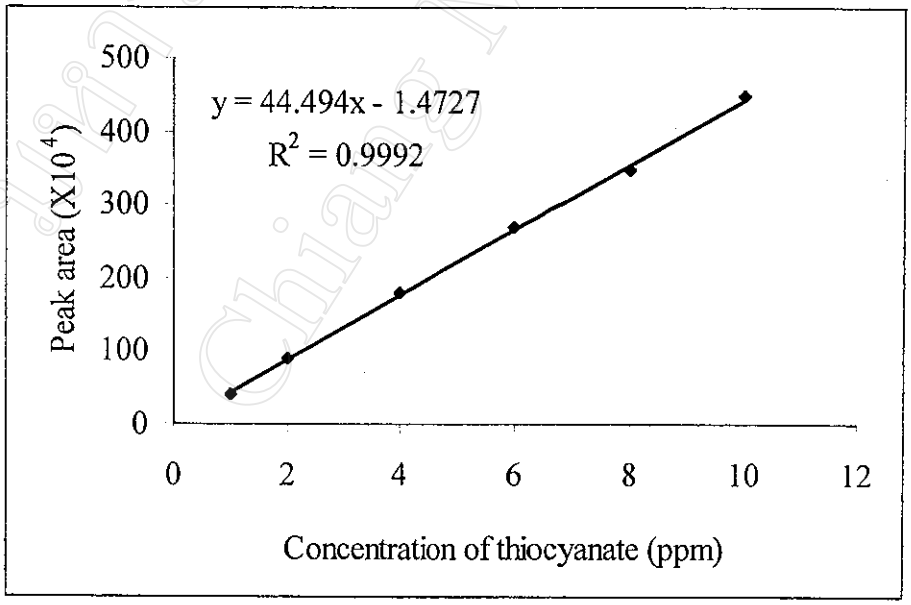

Figure 3.29 Calibration curve of thiocyanate in water sample used for calculating % recovery.

Table 3.26 % Recovery of SCN^- in water sample when spiked with standard SCN^- at various concentrations

Spiked standard SCN^- (ppm)	Peak area ($x10^4$) (arbitrary unit)	Concentration (ppm)	% Recovery
0.00	0	0	-
1.00	42.225	0.98	98.2
2.00	82.731	1.89	94.5
3.00	127.283	2.89	96.3
4.00	177.836	4.03	100.8
Average			97.4

Percent recovery check was accomplished by using the spike method. The result of percent recovery were 99.8 for IO_3^-, 98.4 for BrO_3^-, 96.8 for NO_3^-, 98.0 for I^- and 97.4 for SCN^-. It indicated that the chromatographic conditions used for the analysis provided an acceptable result. **Figure 3.30-3.31** shows example chromatograms of tap water samples spiked with IO_3^-, BrO_3^-, NO_3^-, I^- and SCN^- in comparison.

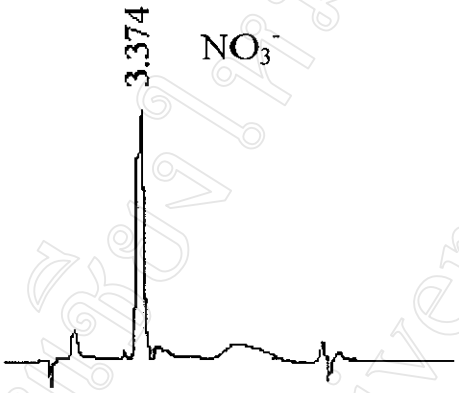

Figure 3.30 Chromatogram of tap water sample; without a spike.

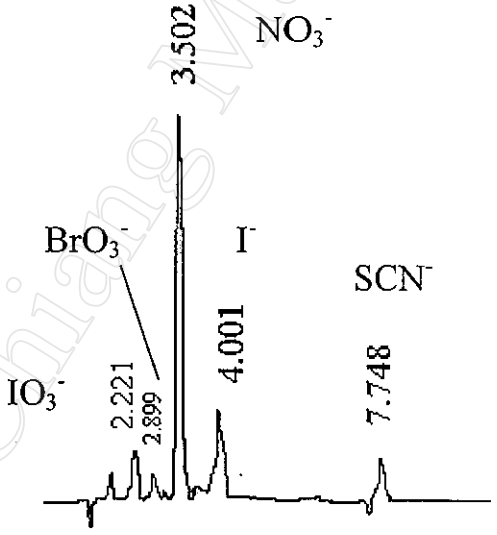

Figure 3.31 Chromatogram of tap water sample; spiked with 1 ppm of each anion.

3.2.5 Analysis of the anions

The water samples collected from the Female Student Dormitories, Chiang Mai University and Phitsanuloke were injected into the ion interaction chromatographic system. The injection volume was 20 μL. By triplicately injecting the sample under the optimum conditions: 5.0 mM heptylamine-phosphate, 5% MeOH (v/v) at pH 6.4±0.3 with a flow rate 0.5 mL/min and wavelength of detection 200 nm. The separating column used was Microsorb MV-100 C_{18} (3μm, 4.6 x 50 mm). The result of the analysis of each water sample is shown in **Table 3.27**.

It is clearly seen from the result in **Table 3.27** that iodate, bromate, iodide and thiocyanate were not found in drinking and tap water samples, only the nitrate was found in all analyzed samples. The chromatogram of tap water sample numbered 4 in **Figure 3.32** is the evidence representing the existence of only nitrate ion in the water samples. The concentration of nitrate present in all the samples were calculated from the standard calibration curve in **Figure 3.27**.

Table 3.27 The amount of anions found in water sample (n=3)

Sample	Amount of anion found (ppm)				
	Iodate	Bromate	Nitrate	Iodide	Thiocyanate
Drinking water 1	ND	ND	0.41	ND	ND
Drinking water 2	ND	ND	0.42	ND	ND
Tap water 1	ND	ND	0.73	ND	ND
Tap water 2	ND	ND	0.96	ND	ND
Tap water 3	ND	ND	1.32	ND	ND
Tap water 4	ND	ND	2.73	ND	ND

ND = Not detectable

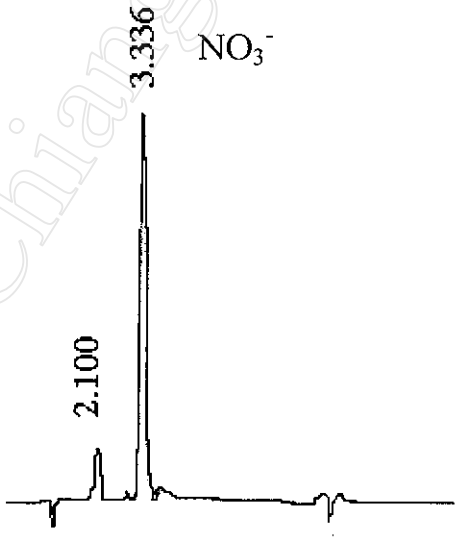

Figure 3.32 Chromatogram of tap water sample 4.